Hindawi
Mathematical Problems in Engineering
Volume 2021, Article ID 2501842, 21 pages
https://doi.org/10.1155/2021/2501842

Research Article

MHD Three-Dimensional Free Convective Flow with Periodic Permeability and Heat Transfer of a Second-Grade Fluid

Atifa Latif,[1,2] **Muhammad Afzal Rana**,[1] **Babar Ahmad**,[3] **and Muhammad Hussan**[2]

[1]*Department of Mathematics & Statistics, Riphah International University, Sector I-14, Islamabad, Pakistan*
[2]*Department of Mathematics, GC University Faisalabad, Faisalabad, Pakistan*
[3]*Department of Mathematics COMSATS University, Islamabad, Pakistan*

Correspondence should be addressed to Atifa Latif; aatifalatif@gmail.com

Received 4 August 2020; Revised 20 January 2021; Accepted 29 January 2021; Published 17 February 2021

Academic Editor: Alessandro Mauro

The present study delivers the mathematical model and theoretical analysis of a three-dimensional flow in a free convection for an electrically conducting incompressible second-grade fluid through a very high porous medium circumscribed by an infinite vertical porous plate subject to a constant suction. A uniform magnetic field along the normal to the surface of plate is applied. Periodic permeability for the medium is assumed, while velocity of free stream is taken to be uniform. Analytic expressions are presented for velocity and temperature fields, pressure, and skin friction components by perturbation technique. The impacts on these physical quantities by the physical parameters existing in the model are discussed and envisioned graphically. It is interesting to note that elastic and permeability parameters are able to control the skin friction along the main flow direction, magnetic field to reduce the pressure, and Reynolds number to control the thermal boundary layer thickness. It is also noted that temperature distribution does not depend upon permeability parameter.

1. Introduction

The study of porous medium in context of free convective flow frequently has fascinated the researches over the last decades. This area has appealing quality due to its wide spread applications in the field of science, technology, and engineering. For example, the processes of purification and filtration in the arena of chemical engineering, the study of seeping water in the river basin, underground water resources in agriculture engineering, and evaporative cooling air conditioners in context of technology are few practical models of porosity in daily routine. Raptis [1] elaborated a free convective time free Newtonian fluid flow past porous medium, and Raptis and Perdikis [2] investigated oscillatory free convective flow of a Newtonian fluid past porous medium.

In the above cited work, both permeability and suction of the porous medium have been supposed to be constant or transient. Since a porous medium, in general, is not a homogeneous channel, there can exist several inhomogeneities in such mediums. Thus, it may not be necessary to consider the permeability or suction of the porous medium as constant. Several efforts [3–6] by Singh et al. have been done in this regard on the motion of Newtonian fluids in three dimensions with periodic variation of permeability or suction velocity passing through an extremely high porous medium. Further, Vafai and Hadim [7] took an overview of the studies of heat transfer in porous beds with natural convection and mixed convection applications. Jain et al. [8] delivered the impact of free convective temperature and sinusoidal permeability of 3-dimensional Newtonian fluid flow past a porous medium with the existence of slip on flow parameters.

Moreover, in the above studies the fluid flows were supposed electrically nonconducting. However, magnetic fields influence many natural and man-made flows. They are routinely used in industries to heat, pump, stir, and levitate liquid metals. There is the terrestrial magnetic field which is maintained by fluid motion in the earth's core, the solar magnetic field which generates sunspots and solar flares, and

the galactic field which influences the formation of stars. The flow problems of an electrically conducting fluid under the influence of magnetic field have attracted the interest of many authors in view of their applications to geophysics, astrophysics, and engineering, and to the boundary layer control in the field of aerodynamics. Ahmed [9] put forward getting the effects of electrically conducted fluid for mixed convective flows with periodic suction velocity and magnetic field through porous vertical plate. Reddy et al. [10] observed that the velocity of 3-dimensional fluid past a porous medium with sinusoidal permeability reduces due to magnetohydrodynamic flow, and the parameter of heat absorption causes enhancing the heat transfer coefficient. Various workers [11–14] analyzed viscoelastic fluids in various geometries under distinct physical states. Further, researchers [15–17] investigated electrically conducting viscoelastic fluids over a stretching sheet/in highly porous mediums with the MHD effects and presented very interesting results.

In many practical applications, a situation may arise when slip of particles at the boundary may occur. For example, the surfaces of air-craft and rockets move at a very high altitude, where particles adjacent to the surface possess a finite tangential velocity which slips along the surface. Seth et al. [18–20] studied various non-Newtonian models with slip/hydromagnetic mechanism in free convective flow past a nonlinear stretching surface/through a porous medium. The workers [21–27] reported important results for free convective flows in three dimensions with periodic permeability of non-Newtonian fluids. Arpino with his coauthors [28, 29] analyzed transient thermal natural convection in porous and partially porous channels. Khanafer and Vafai [30] recently investigated porous medium with the applications of nanofluids.

In the present study, a second-grade free convective fluid flow in three dimensions through a very highly porous medium with periodic permeability in the presence of magnetic field is explored. To the author's knowledge, such a study for the second-grade fluid model has not been addressed. This constitutes the novelty of the present analysis. The nondimensional highly nonlinear partial differential equations subject to appropriate boundary conditions are solved analytically using regular perturbation technique. A detailed parametric study of the Hartmann number, permeability parameter, Grashof number, Prandtl number, Reynolds number, and non-Newtonian parameter on velocity components, skin friction components, and the coefficient of heat transfer is visualized graphically. Elaborate interpretation of the physics of the flow is also conducted. In view of the above considerations, the setup of the article is as given below.

Section 2 of the article narrates the description and modeling of the problem, while Section 3 gives solutions of the model in different dimensions for main flow, secondary flow, and energy equation by the regular perturbation technique, friction coefficients along z-direction and x-direction, and the coefficient of heat transfer rate is also demonstrated at the end of this section. Results and discussions are interpreted in Section 4 and conclusions are described in Section 5.

2. Description and Modeling of Problem

The present study is the investigation of a three-dimensional second-grade fluid through an extremely high porous medium circumscribed by an infinite vertical porous plate placed on the xz-plane with x-axis pointing upward along the plate and y-axis pointing along the normal to the plane of the plate (Figure 1) and

$$K(z) = \frac{K_0}{(1 + \varepsilon \cos(\pi z/l))}, \tag{1}$$

is the porous medium periodic permeability, where K_0 presents the medium mean permeability, $\varepsilon (\ll 1)$ is the permeability variation's amplitude, and l is the length of wave for the permeability distribution. The sinusoidal variation in permeability (1) causes the flow to be 3-dimensional. The following assumptions are taken into account:

(i) The fluid is incompressible and the fluid flow is laminar

(ii) All fluid's properties are considered to be constant; however, fluid density variation effect with temperature is contemplated in the term of body force

(iii) A uniform magnetic field $\overrightarrow{B}_0$ is applied along the y-axis

(iv) Magnetic Reynolds number is assumed to be very small so that the induced magnetic field is negligible [31, 32]

(v) The electric field is assumed to be zero

(vi) Suction velocity U and free stream velocity V_0 are constant

The form of velocity field here is taken:

$$\overrightarrow{V} = u(y,z)\mathbf{i} + v(y,z)\mathbf{j} + w(y,z)\mathbf{k}, \tag{2}$$

with velocity components u, v, w, respectively, in the x-, y-, z-directions. The physical quantities will not be x dependent as the plate length is infinite in x-direction and definitely the flow remains in 3 dimensions because of the variation of sinusoidal permeability. Now, consider the equations of motion [33, 34] governing the given fluid flow.

$$\begin{aligned} &\nabla \cdot \overrightarrow{V} = 0, \\ &\rho \frac{\mathrm{d}\overrightarrow{V}}{\mathrm{d}t} = \nabla \cdot \widetilde{\tau} + \rho \overrightarrow{b} + \overrightarrow{J} \times \overrightarrow{B} - \frac{\mu \overrightarrow{V}}{K}, \\ &\rho \frac{\mathrm{d}\varrho}{\mathrm{d}t} = -\nabla \cdot \overrightarrow{q}, \end{aligned} \tag{3}$$

where $\widetilde{\tau}$, a Cauchy stress tensor for the second-grade fluid [35], is defined below in (4), $\overrightarrow{V}$ is velocity field defined in (2), ∇ is the vector operator, fluid density is ρ, $\overrightarrow{b}$ is the generated body force per unit mass, $\overrightarrow{B}$ is the total magnetic field, $\overrightarrow{J}$ is the electric current density, μ is the dynamic viscosity, $\varrho = c_p T$, $\overrightarrow{q} = -k_t \nabla T$ and T is the temperature, k_t is thermal conductivity, and c_p is specific heat at constant pressure.

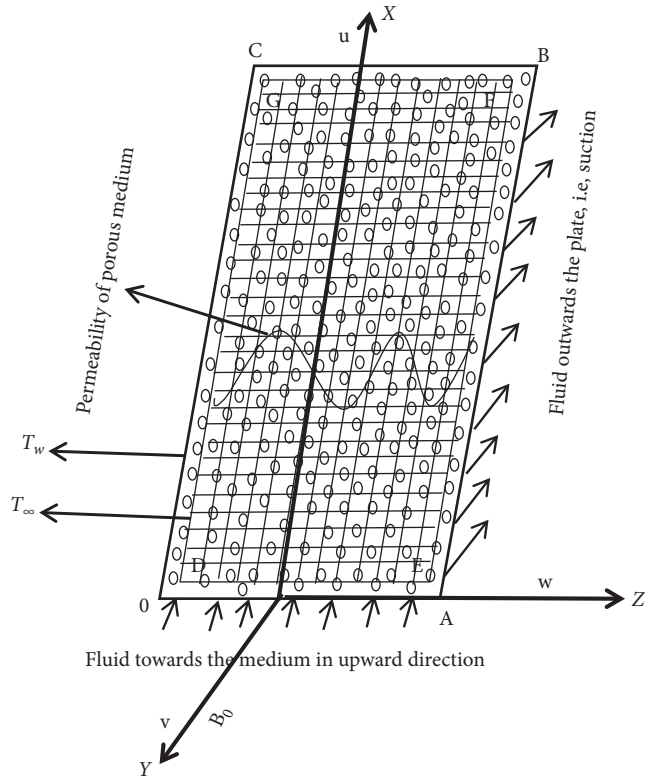

Figure 1: Physical model of the problem.

$$\tilde{\tau} = -p\tilde{I} + \mu\tilde{A}_1 + \alpha_1\tilde{A}_2 + \alpha_2\tilde{A}_1^2, \tag{4}$$

where $\tilde{A}_1$ and $\tilde{A}_2$ are Rivlin–Ericksen tensors, defined in equation (5), p is pressure, $\tilde{I}$ is the identity tensor, and α_1 and α_2 are material constants.

$$\begin{aligned} \tilde{A}_1 &= (\operatorname{grad}\vec{V})^T + \operatorname{grad}\vec{V}, \\ \tilde{A}_2 &= \frac{d\tilde{A}_1}{dt} + (\operatorname{grad}\vec{V})^T\vec{A}_1 + \vec{A}_1(\operatorname{grad}\vec{V}). \end{aligned} \tag{5}$$

Now, for model (4) to be compatible with the thermodynamics in the sense that all motions meet the Clausius–Duhem inequality and with the supposition that the specific Helmholtz free energy is a minimum in equilibrium [35], then the following conditions must satisfy the material parameters:

$$\begin{aligned} \alpha_1 + \alpha_2 &= 0, \\ \alpha_1 &\geq 0, \\ \mu &\geq 0. \end{aligned} \tag{6}$$

In the absence of displacement currents, Maxwell's equations modified Ohm's law [31, 32] can be written as

$$\begin{aligned} \nabla\cdot\vec{B} &= 0, \\ \nabla\times\vec{B} &= \mu_m\vec{J}, \\ \nabla\times\vec{E} &= -\frac{\partial\vec{B}}{\partial t}, \\ \vec{J} &= \sigma\left[\vec{E} + \vec{V}\times\vec{B}\right], \end{aligned} \tag{7}$$

where μ_m is the magnetic permeability, σ is the electrical conductivity of the fluid, and $\vec{E}$ is the electric field. Using the usual Boussinesq assumption for the body force [33], we have

$$\rho\vec{b} = -\rho_0[1 - \beta_0(T - T_\infty)]g, \tag{8}$$

where g denotes the gravity, β_0 the coefficient of thermal expansion, T_∞ reference temperature, and ρ_0 a constant density which is going to symbolize as ρ throughout the article for convenience. The problem defined in equation (3) can be restraint in the following mathematical model with the support of equations (1)–(8).

$$\frac{\partial v}{\partial y}+\frac{\partial w}{\partial z}=0, \tag{9}$$

$$\begin{aligned}\rho\left(v\frac{\partial u}{\partial y}+w\frac{\partial u}{\partial z}\right)&=g\rho\beta_0\left(T-T_\infty\right)+\mu\left[\frac{\partial^2 u}{\partial y^2}+\frac{\partial^2 u}{\partial z^2}\right]-\sigma B_0^2 u\\&\quad+\alpha_1\left[v\frac{\partial^3 u}{\partial y^3}+w\frac{\partial^3 u}{\partial y^2\partial z}+w\frac{\partial^3 u}{\partial z^3}+v\frac{\partial^3 u}{\partial y\partial z^2}\right]-\frac{\mu}{K}\left(u-U\right),\end{aligned} \tag{10}$$

$$\rho\left(v\frac{\partial v}{\partial y}+w\frac{\partial v}{\partial z}\right)=-\frac{\partial p}{\partial y}+\mu\left[\frac{\partial^2 v}{\partial y^2}+\frac{\partial^2 v}{\partial z^2}\right]+\alpha_1\begin{bmatrix}v\dfrac{\partial^3 v}{\partial y^3}+w\dfrac{\partial^3 v}{\partial y^2\partial z}+v\dfrac{\partial^3 v}{\partial y\partial z^2}+w\dfrac{\partial^3 v}{\partial z^3}+\dfrac{\partial v}{\partial z}\dfrac{\partial^2 v}{\partial y\partial z}\\+\dfrac{\partial u}{\partial z}\dfrac{\partial^2 u}{\partial y\partial z}+5\dfrac{\partial v}{\partial y}\dfrac{\partial^2 v}{\partial y^2}+\dfrac{\partial v}{\partial z}\dfrac{\partial^2 w}{\partial y^2}+2\dfrac{\partial u}{\partial y}\dfrac{\partial^2 u}{\partial y^2}\\+2\dfrac{\partial w}{\partial y}\dfrac{\partial^2 w}{\partial y^2}+\dfrac{\partial u}{\partial y}\dfrac{\partial^2 u}{\partial z^2}+\dfrac{\partial v}{\partial y}\dfrac{\partial^2 v}{\partial z^2}\end{bmatrix}-\frac{\mu}{K}v, \tag{11}$$

$$\begin{aligned}\rho\left(v\frac{\partial w}{\partial y}+w\frac{\partial w}{\partial z}\right)&=-\frac{\partial p}{\partial z}+\mu\left[\frac{\partial^2 w}{\partial y^2}+\frac{\partial^2 w}{\partial z^2}\right]-\sigma B_0^2 w\\&\quad+\alpha_1\begin{bmatrix}w\dfrac{\partial^3 w}{\partial y^2\partial z}+v\dfrac{\partial^3 w}{\partial y^3}+v\dfrac{\partial^3 w}{\partial y\partial z^2}+w\dfrac{\partial^3 w}{\partial z^3}+\dfrac{\partial w}{\partial y}\dfrac{\partial^2 w}{\partial y\partial z}\\+\dfrac{\partial u}{\partial y}\dfrac{\partial^2 u}{\partial y\partial z}+5\dfrac{\partial w}{\partial z}\dfrac{\partial^2 w}{\partial z^2}+\dfrac{\partial w}{\partial y}\dfrac{\partial^2 v}{\partial z^2}+2\dfrac{\partial u}{\partial z}\dfrac{\partial^2 u}{\partial z^2}\\+2\dfrac{\partial v}{\partial z}\dfrac{\partial^2 v}{\partial z^2}+\dfrac{\partial u}{\partial z}\dfrac{\partial^2 u}{\partial y^2}+\dfrac{\partial w}{\partial z}\dfrac{\partial^2 w}{\partial y^2}\end{bmatrix}-\frac{\mu}{K}w,\end{aligned} \tag{12}$$

$$\rho\left(v\frac{\partial T}{\partial y}+w\frac{\partial T}{\partial z}\right)=\frac{k_t}{c_p}\left[\frac{\partial^2 T}{\partial y^2}+\frac{\partial^2 T}{\partial z^2}\right], \tag{13}$$

with the boundary conditions [6].

$$\left.\begin{aligned}&\text{When } y=0, \quad v=-V_0, \quad T=T_w, \quad u=0, \quad w=0,\\&\text{At } y\longrightarrow\infty, \quad p=p_\infty, \quad T=T_\infty, \quad u=U, \quad w=0,\end{aligned}\right\} \tag{14}$$

where V_0 is a positive constant suction velocity and -ve sign arises because of the suction towards plate, and the constant pressure in free stream is denoted as p_∞ while plate temperature and the fluid temperature (far away from the plate) both are, respectively, T_w and T_∞. Now, the variables are assigned the following dimensionless values:

$$\left.\begin{aligned} Uu^{\triangleright} &= u, \\ ly^{\triangleright} &= y, \\ lz^{\triangleright} &= z, \\ V_0 v^{\triangleright} &= v, \\ V_0 w^{\triangleright} &= w, \\ \rho V_0^2 p^{\triangleright} &= p, \\ l^2 K_0^{\triangleright} &= K_0, \\ \theta &= \frac{T - T_\infty}{T_w - T_\infty}, \end{aligned}\right\} \tag{15}$$

where the nondimensional variables are $u^{\triangleright}, v^{\triangleright}, w^{\triangleright}, y^{\triangleright}, z^{\triangleright}, p^{\triangleright}$, and $K_0^{\triangleright}$. Then, after the omission of symbol "$\triangleright$",equations (9)-(14) have the following form for ease:

$$\frac{\partial v}{\partial y} + \frac{\partial w}{\partial z} = 0, \tag{16}$$

$$v\frac{\partial u}{\partial y} + w\frac{\partial u}{\partial z} = G\mathrm{Re}\theta - \frac{1}{\mathrm{Re}K_0}(1 + \varepsilon\cos\pi z)(u-1) + \frac{1}{\mathrm{Re}}\left[\frac{\partial^2 u}{\partial y^2} + \frac{\partial^2 u}{\partial z^2}\right] - \mathrm{Mu} + L\left[v\frac{\partial^3 u}{\partial y^3} + w\frac{\partial^3 u}{\partial y^2 \partial z} + w\frac{\partial^3 u}{\partial z^3} + v\frac{\partial^3 u}{\partial y \partial z^2}\right], \tag{17}$$

$$v\frac{\partial v}{\partial y} + w\frac{\partial v}{\partial z} = -\frac{\partial p}{\partial y} - \frac{1}{\mathrm{Re}K_0}(1 + \varepsilon\cos\pi z)v + \frac{1}{\mathrm{Re}}\left[\frac{\partial^2 v}{\partial y^2} + \frac{\partial^2 v}{\partial z^2}\right] + L\begin{bmatrix} v\dfrac{\partial^3 v}{\partial y^3} + w\dfrac{\partial^3 v}{\partial y^2 \partial z} + v\dfrac{\partial^3 v}{\partial y \partial z^2} + w\dfrac{\partial^3 v}{\partial z^3} + \dfrac{\partial v}{\partial z}\dfrac{\partial^2 v}{\partial y \partial z} \\ +\alpha^2\dfrac{\partial u}{\partial z}\dfrac{\partial^2 u}{\partial y \partial z} + 5\dfrac{\partial v}{\partial y}\dfrac{\partial^2 v}{\partial y^2} + \dfrac{\partial v}{\partial z}\dfrac{\partial^2 w}{\partial y^2} + 2\alpha^2\dfrac{\partial u}{\partial y}\dfrac{\partial^2 u}{\partial y^2} \\ +2\dfrac{\partial w}{\partial y}\dfrac{\partial^2 w}{\partial y^2} + \alpha^2\dfrac{\partial u}{\partial y}\dfrac{\partial^2 u}{\partial z^2} + \dfrac{\partial v}{\partial y}\dfrac{\partial^2 v}{\partial z^2} \end{bmatrix}, \tag{18}$$

$$v\frac{\partial w}{\partial y} + w\frac{\partial w}{\partial z} = -\frac{\partial p}{\partial z} - \frac{1}{\mathrm{Re}K_0}(1 + \varepsilon\cos\pi z)w + \frac{1}{\mathrm{Re}}\left[\frac{\partial^2 w}{\partial y^2} + \frac{\partial^2 w}{\partial z^2}\right] - Mw + L\begin{bmatrix} w\dfrac{\partial^3 w}{\partial y^2 \partial z} + v\dfrac{\partial^3 w}{\partial y^3} + v\dfrac{\partial^3 w}{\partial y \partial z^2} + w\dfrac{\partial^3 w}{\partial z^3} + \dfrac{\partial w}{\partial y}\dfrac{\partial^2 w}{\partial y \partial z} \\ +\alpha^2\dfrac{\partial u}{\partial y}\dfrac{\partial^2 u}{\partial y \partial z} + 5\dfrac{\partial w}{\partial z}\dfrac{\partial^2 w}{\partial z^2} + \dfrac{\partial w}{\partial y}\dfrac{\partial^2 v}{\partial z^2} + 2\alpha^2\dfrac{\partial u}{\partial z}\dfrac{\partial^2 u}{\partial z^2} \\ +2\dfrac{\partial v}{\partial z}\dfrac{\partial^2 v}{\partial z^2} + \alpha^2\dfrac{\partial u}{\partial z}\dfrac{\partial^2 u}{\partial y^2} + \dfrac{\partial w}{\partial z}\dfrac{\partial^2 w}{\partial y^2} \end{bmatrix}, \tag{19}$$

$$v\frac{\partial \theta}{\partial y} + w\frac{\partial \theta}{\partial z} = \frac{1}{\mathrm{RePr}}\left[\frac{\partial^2 \theta}{\partial y^2} + \frac{\partial^2 \theta}{\partial z^2}\right], \tag{20}$$

and the associated boundary conditions are

$$\left.\begin{aligned} &\text{As } y \longrightarrow \infty\text{: } \theta = 0, \quad u = 1, \quad w = 0, \quad p = p_\infty, \\ &\text{For } y = 0\text{: } \theta = 1, \qquad u = 0, \quad w = 0, \quad v = -1, \end{aligned}\right\} \tag{21}$$

where Reynolds number, Grashof number, elastic parameter, Prandtl number, magnetic parameter, and suction parameter, respectively, are given below:

$$\begin{aligned} \mathrm{Re} &= \frac{V_0 l}{\nu}, \\ G &= \frac{\nu g \beta_0 (T_w - T_\infty)}{U V_0^2}, \\ L &= \frac{\alpha_1}{\rho l^2}, \\ \mathrm{Pr} &= \frac{\mu c_p}{k_t}, \\ M &= \frac{\sigma B_0^2 l}{\rho V_0}, \\ \alpha &= \frac{U}{V_0}. \end{aligned} \tag{22}$$

3. Analysis of the Mathematical Model

In this section, we discuss the solutions of equations (16)–(20) in two and three dimensions so we assume the following type of a solution in the neighbourhood of the channel:

$$g = g_0 + \varepsilon g_1 + \varepsilon^2 g_2 + \cdots, \tag{23}$$

where g takes the position for all of θ, p, u, v, and w and ε is a very small parameter.

3.1. Two-Dimensional Solution. For $\varepsilon = 0$, the problem becomes two-dimensional and consequently, we have

$$\frac{dv_0}{dy} = 0, \tag{24}$$

$$L\frac{d^3u_0}{dy^3} - \frac{1}{\mathrm{Re}}\frac{d^2u_0}{dy^2} - \frac{du_0}{dy} + \left(\frac{1}{\mathrm{Re}K_0} + M\right)u_0 = \frac{1}{\mathrm{Re}K_0} + G\mathrm{Re}\theta_0, \tag{25}$$

$$2L\alpha^2\frac{du_0}{dy}\frac{d^2u_0}{dy^2} + 2L\frac{dw_0}{dy}\frac{d^2w_0}{dy^2} + \frac{1}{\mathrm{Re}K_0} = \frac{dp_0}{dy}, \tag{26}$$

$$L\mathrm{Re}\frac{d^3w_0}{dy^3} + \frac{d^2w_0}{dy^2} + \mathrm{Re}\frac{dw_0}{dy} - \left(\frac{1}{K_0} + M\mathrm{Re}\right)w_0 = 0, \tag{27}$$

$$\frac{d^2\theta_0}{dy^2} + \mathrm{RePr}\frac{d\theta_0}{dy} = 0, \tag{28}$$

subject to boundary conditions

$$\left.\begin{aligned} &\theta_0 = 1, \quad u_0 = 0, \quad v_0 = -1, \quad w_0 = 0, \text{ at } y = 0, \\ &\theta_0 = 0, \quad u_0 = 1, \quad w_0 = 0, \quad p_0 = p_\infty \text{ as } y \longrightarrow \infty. \end{aligned}\right\} \tag{29}$$

Clearly, due to the presence of elasticity parameter in equations (25)–(27), the order of these differential equations has increased from 2 to 3. For unique solution of equations (25)–(27), three boundary conditions are required here. To take off this difficulty, consider the solution of the following type:

$$u_{00} + Lu_{01} + O\left(L^2\right) = u_0, \tag{30}$$

taking the parameter L very small. Solving the equations (24) and (26)–(28), we get the following solutions:

$$\begin{aligned} v_0 &= -1, \\ w_0 &= 0, \\ p_0 &= p_\infty, \\ \theta_0 &= e^{-\mathrm{RePr}y}. \end{aligned} \tag{31}$$

Solving equation (25) with the help of equation (30) and comparing coefficients of order of L^0 and L, we obtain the following boundary value problems:

$$\left.\begin{aligned} &\frac{d^2u_{00}}{dy^2} + \mathrm{Re}\frac{du_{00}}{dy} - \left(\frac{1}{K_0} + M\mathrm{Re}\right)u_{00} = -\frac{1}{K_0} - G\mathrm{Re}^2 e^{-\mathrm{RePr}y}, \\ &u_{00}(0) = 0, \\ &u_{00}(\infty) = 1, \end{aligned}\right\} \tag{32}$$

$$\left.\begin{aligned} &\mathrm{Re}\frac{d^3u_{00}}{dy^3} - \frac{d^2u_{01}}{dy^2} - \mathrm{Re}\frac{du_{01}}{dy} + \left(\frac{1}{K_0} + M\mathrm{Re}\right)u_{01} = 0, \\ &u_{01}(0) = 0, \\ &u_{01}(\infty) = 0. \end{aligned}\right\} \tag{33}$$

Solving the boundary value problems (32) and (33), then the zeroth-order solution yields

$$u_0(y) = \left(G\lambda_0 - \frac{1}{1 + K_0 M\mathrm{Re}}\right)e^{-\lambda y} + \frac{1}{1 + K_0 M\mathrm{Re}} - G\lambda_0 e^{-\mathrm{RePr}y} + LG\lambda_0^2\mathrm{Re}^2\mathrm{Pr}^3\left(e^{-\mathrm{RePr}y} - e^{-\lambda y}\right). \tag{34}$$

Results of [6, 21] are retrieved for $M = 0$ and for both $M = 0 = L$, respectively.

3.2. Three-Dimensional Solution. For $\varepsilon \neq 0$, the flow turns into three-dimensional and solution of the type described in equation (23) can be taken as the assumed solution of the obtaining expression. Then by comparing first-order terms of ε, we acquired the following partial differential equations from equations (16)–(20):

$$\frac{\partial v_1}{\partial y} + \frac{\partial w_1}{\partial z} = 0, \tag{35}$$

$$-\frac{\partial u_1}{\partial y} + v_1\frac{\partial u_0}{\partial y} = G\mathrm{Re}\theta_1 - \left(\frac{1}{\mathrm{Re}K_0} + M\right)u_1 + \frac{1}{\mathrm{Re}}\left(\frac{\partial^2 u_1}{\partial y^2} + \frac{\partial^2 u_1}{\partial z^2}\right) + L\left(-\frac{\partial^3 u_1}{\partial y^3} - \frac{\partial^3 u_1}{\partial y \partial z^2} + v_1\frac{\partial^3 u_0}{\partial y^3}\right) - \frac{1}{\mathrm{Re}K_0}(u_0 - 1)\cos\pi z, \tag{36}$$

$$-\frac{\partial v_1}{\partial y} = -\frac{\partial p_1}{\partial y} + \frac{1}{\mathrm{Re}}\left(\frac{\partial^2 v_1}{\partial y^2} + \frac{\partial^2 v_1}{\partial z^2}\right) - L\left(\frac{\partial^3 v_1}{\partial y^3} + \frac{\partial^3 v_1}{\partial y \partial z^2}\right) - \frac{1}{\mathrm{Re}K_0}(v_1 - \cos\pi z), \tag{37}$$

$$-\frac{\partial w_1}{\partial y} = -\frac{\partial p_1}{\partial z} + \frac{1}{\mathrm{Re}}\left(\frac{\partial^2 w_1}{\partial y^2} + \frac{\partial^2 w_1}{\partial z^2}\right) - L\left(\frac{\partial^3 w_1}{\partial y^3} + \frac{\partial^3 w_1}{\partial y \partial z^2}\right) - \left(\frac{1}{\mathrm{Re}K_0} + M\right)w_1, \tag{38}$$

$$-\frac{\partial \theta_1}{\partial y} + v_1\frac{\partial \theta_0}{\partial y} = \frac{1}{\mathrm{RePr}}\left(\frac{\partial^2 \theta_1}{\partial y^2} + \frac{\partial^2 \theta_1}{\partial z^2}\right). \tag{39}$$

Similarly, the boundary conditions (21) yield

$$\left.\begin{aligned} &\text{At } y = 0, && u_1 = 0 = v_1 = w_1 = \theta_1, \\ &\text{As } y \longrightarrow \infty, && u_1 = 0 = w_1 = \theta_1, \quad p_1 = 0. \end{aligned}\right\} \tag{40}$$

The set of coupled PDEs (partial differential equations) subject to the boundary conditions from (35)–(40) describes the 3-dimensional free convective fluid flow.

3.3. Solution of Cross Flow. To get the solutions of PDEs (35)–(39), we explore the equations (35), (37), and (38) firstly as these three equations are independent of temperature field and main flow.

Let us suppose the solutions for p_1, v_1, and w_1 as

$$\begin{aligned} p_1(y,z) &= p_{11}(y)\cos\pi z, \\ v_1(y,z) &= -v_{11}(y)\cos\pi z, \\ w_1(y,z) &= \frac{1}{\pi}v_{11}'(y)\sin\pi z, \end{aligned} \tag{41}$$

where $v_{11}'(y)$ is the derivative. All the equations in (41) satisfy the continuity equation (35). Putting values from equations (41) into equations (37) and (38), we have

$$L\mathrm{Re}v_{11}'' - v_{11}'' - \left(L\pi^2 + 1\right)\mathrm{Re}v_{11}' + \left(\pi^2 + \frac{1}{K_0}\right)v_{11} = \mathrm{Re}p_{11}' - \frac{1}{K_0}, \tag{42}$$

$$L\mathrm{Re}v_{11}^{iv} - v_{11}'' - \left(L\pi^2 + 1\right)\mathrm{Re}v_{11}'' + \left(\pi^2 + \frac{1}{K_0} + M\mathrm{Re}\right)v_{11}' = \pi^2\mathrm{Re}p_{11}, \tag{43}$$

with the boundary conditions

$$\begin{aligned} v_{11}'(\infty) &= 0, \\ v_{11}(0) &= 0, \\ v_{11}'(0) &= 0. \end{aligned} \tag{44}$$

Simultaneously solving both equations (42) and (43) and eliminating p_{11}, the pressure term, we obtain the following differential equation:

$$L\mathrm{Re}v_{11}^{v} - v_{11}^{iv} - \left(2L\pi^2 + 1\right)\mathrm{Re}v_{11}'' + \left(2\pi^2 + \frac{1}{K_0} + M\mathrm{Re}\right)v_{11}'' + \pi^2\left(L\pi^2 + 1\right)\mathrm{Re}v_{11}' - \pi^2\left(\pi^2 + \frac{1}{K_0}\right)v_{11} = \frac{\pi^2}{K_0}, \tag{45}$$

and equation (45) can be solved by the perturbation technique, assuming the following solution for equation (45) with a very small parameter L:

$$v_{11} = v_{00} + Lv_{01} + O\left(L^2\right). \tag{46}$$

Putting equations (46) in equations (45) and (44), comparing like powers of L, and then solving the resulting boundary value problems, we obtain

$$v_{11} = \frac{-d_2e^{d_1y} + d_1e^{d_2y} - d_1 + d_2}{\left(d_1 - d_2\right)\left(\pi^2K_0 + 1\right)}(1 + L), \tag{47}$$

where d_1 and d_2 are the real roots of equation (45) having long expressions that are not shown here for the sake of brevity. In view of (23), (31), and (41), finally we get

$$v(y,z) = -1 + \varepsilon\frac{-d_2e^{d_1y} + d_1e^{d_2y} - d_1 + d_2}{\left(d_1 - d_2\right)\left(\pi^2K_0 + 1\right)}(1 + L)\cos\pi z, \tag{48}$$

$$w(y,z) = \frac{\varepsilon(1 + L)d_1d_2}{\pi\left(d_1 - d_2\right)\left(\pi^2K_0 + 1\right)}\left(e^{d_2y} - e^{d_1y}\right)\sin\pi z. \tag{49}$$

3.4. Temperature Field and Pressure. The value of pressure can be obtained by using equations (23), (31), (41), (43), and (48), which is given by

$$p(y,z) = p_\infty + \frac{\varepsilon(1 + L)d_1d_2\cos\pi z}{\pi^2\mathrm{Re}\left(d_1 - d_2\right)\left(\pi^2K_0 + 1\right)} \times \begin{pmatrix} \left(-L\mathrm{Re}d_1^3 + d_1^2 + \left(L\pi^2 + 1\right)\mathrm{Re}d_1 - \pi^2 - \frac{1}{K_0} - M\mathrm{Re}\right)e^{d_1y} \\ + \left(L\mathrm{Re}d_2^3 - d_2^2 - \left(L\pi^2 + 1\right)\mathrm{Re}d_2 + \pi^2 + \frac{1}{K_0} + M\mathrm{Re}\right)e^{d_2y} \end{pmatrix}. \tag{50}$$

Now, assume the following solution for getting the result of temperature distribution:

$$\theta_1(y,z) = \theta_{11}(y)\cos\pi z. \tag{51}$$

Then, PDE (39) with the boundary conditions

$$\begin{aligned} \theta_{11}(\infty) &= 0, \\ \theta_{11}(0) &= 0, \end{aligned} \tag{52}$$

yields

$$\theta(y,z) = e^{-\mathrm{RePr}y} + \frac{\varepsilon\mathrm{Re}^2\mathrm{Pr}^2(1 + L)\cos\pi z}{\left(d_1 - d_2\right)\left(\pi^2K_0 + 1\right)} \cdot \left(\left(A - B + \frac{d_1 - d_2}{\pi^2}\right)e^{-\beta y} + Ae^{\left(d_1 - \mathrm{RePr}\right)y} + Be^{\left(d_2 - \mathrm{RePr}\right)y} + \frac{d_1 - d_2}{\pi^2}e^{-\mathrm{RePr}y}\right), \tag{53}$$

where $A = (-d_2/d_1^2 - d_1\mathrm{RePr} - \pi^2)$, $B = (d_1/d_2^2 - d_2\mathrm{RePr} - \pi^2)$, $\lambda_0 = (\mathrm{Re}^2/\mathrm{Re}^2\mathrm{Pr}(\mathrm{Pr}-1)) - ((1/K_0) + M\mathrm{Re}))$, $\lambda = (\mathrm{Re}/2) + \sqrt{(\mathrm{Re}/2)^2 + (1/K_0) + M\mathrm{Re}}$, $\lambda_1 = (\mathrm{Re}/2) + \sqrt{(\mathrm{Re}/2)^2 + \pi^2 + (1/K_0) + M\mathrm{Re}}$, $\beta = (\mathrm{RePr}/2) + \sqrt{(\mathrm{RePr}/2)^2 + \pi^2}$.

3.5. Solution of Main Flow. Now, finally the solution of main flow can be acquired from the partial differential equation (36). Similar to the previous solutions, we assume

$$u_1(y,z) = u_{11}(y)\cos\pi z, \tag{54}$$

as the solution for (36), and for perturbation on small parameter L, we take

$$u_{11} = u_{100} + Lu_{110} + O\left(L^2\right). \tag{55}$$

Subsequently computing, we have the result

$$\begin{aligned} u_{100}(y) &= \left(A_1 + A_2 + A_{11}\right)e^{-\lambda_1 y} - A_1 e^{-\lambda y} - A_2 e^{-\mathrm{RePr}y} - A_{11} \\ &\quad \cdot -\frac{\mathrm{Re}}{\left(d_1 - d_2\right)\left(\pi^2 K_0 + 1\right)}\begin{bmatrix} A_3 e^{-\beta y} + A_4 e^{\left(d_1 - \mathrm{RePr}\right)y} + A_5 e^{\left(d_2 - \mathrm{RePr}\right)y} \\ +A_6 e^{-\mathrm{RePr}y} + A_7 e^{\left(d_1 - \lambda\right)y} - A_8 e^{\left(d_2 - \lambda\right)y} \\ -A_9 e^{-\lambda y} - A_{10} e^{-\lambda_1 y} \end{bmatrix}, \end{aligned} \tag{56}$$

$$\begin{aligned} u_{110}(y) &= \left(B_3 - B_2\right)e^{-\lambda_1 y} - B_2 e^{-\lambda y} + B_3 e^{-\mathrm{RePr}y} \\ &\quad + \frac{\mathrm{Re}}{\left(d_1 - d_2\right)\left(\pi^2 K_0 + 1\right)}\begin{bmatrix} B_4 e^{-\beta y} + B_5 e^{\left(d_1 - \mathrm{RePr}\right)y} + B_6 e^{\left(d_2 - \mathrm{RePr}\right)y} \\ +B_7 e^{-\mathrm{RePr}y} + B_8 e^{\left(d_1 - \lambda\right)y} + B_9 e^{\left(d_2 - \lambda\right)y} \\ -B_{10} e^{-\lambda y} - B_{11} e^{-\lambda_1 y} \end{bmatrix}, \end{aligned} \tag{57}$$

and equations (56) and (57) in view of equations (55), (54), and (23) attain the final solution for main flow velocity. It is good to reveal that the results of both [6, 21] are successfully retrieved for $L = 0 = M$ and $M = 0$, respectively. The constants of integration that involved the solutions of (56) and (57) are as follows:

$$
\begin{aligned}
A_1 &= \frac{G\lambda_0 - 1}{K_0\pi^2},\\
A_2 &= \frac{G\lambda_0}{K_0\left[\mathrm{Re}^2\mathrm{Pr}\left(\mathrm{Pr}-1\right) - \left(\pi^2 + \left(1/K_0\right) + M\mathrm{Re}\right)\right]},\\
A_3 &= \frac{G\mathrm{Re}^3\mathrm{Pr}^2\left(A + B + \left(d_1 - d_2/\pi^2\right)\right)}{\beta^2 - \mathrm{Re}\beta - \left(\pi^2 + \left(1/K_0\right) + M\mathrm{Re}\right)},\\
A_4 &= \frac{G\mathrm{RePr}\left(\mathrm{R}^2\mathrm{ePr}A - \lambda_0 d_2\right)}{\left(d_1 - \ \mathrm{RePr}\right)^2 + R_e\left(d_1 - \mathrm{RePr}\right) - \left(\pi^2 + \left(1/K_0\right) + M\mathrm{Re}\right)},\\
A_5 &= \frac{G\mathrm{RePr}\left(\mathrm{Re}^2\mathrm{Pr}B - \lambda_0 d_1\right)}{\left(d_2 - \ \mathrm{RePr}\right)^2 + \mathrm{Re}\left(d_2 - \mathrm{RePr}\right) - \left(\pi^2 + \left(1/K_0\right) + M\mathrm{Re}\right)},\\
A_6 &= \frac{G\mathrm{RePr}\left(d_1 - d_2\right)\left(\left(\mathrm{Re}^2\mathrm{Pr}/\pi^2\right) - \lambda_0\right)}{\mathrm{Re}^2\mathrm{Pr}\left(\mathrm{Pr}-1\right) - \left(\pi^2 + \left(1/K_0\right) + M\mathrm{Re}\right)},\\
A_7 &= \frac{\lambda d_2\left(G\lambda_0 - \left(1/\left(1 + K_0 M\mathrm{Re}\right)\right)\right)}{\left(d_1 - \ \lambda\right)^2 + \mathrm{Re}\left(d_1 - \lambda\right) - \left(\pi^2 + \left(1/K_0\right) + M\mathrm{Re}\right)},\\
A_8 &= \frac{\lambda d_1\left(G\lambda_0 - \left(1/\left(1 + K_0 M\mathrm{Re}\right)\right)\right)}{\left(d_2 - \ \lambda\right)^2 + \mathrm{Re}\left(d_2 - \lambda\right) - \left(\pi^2 + \left(1/K_0\right) + M\mathrm{Re}\right)},\\
A_9 &= \frac{\lambda\left(d_1 - d_2\right)\left(G\lambda_0 - \left(1/\left(1 + K_0 M\mathrm{Re}\right)\right)\right)}{\pi^2},\\
A_{10} &= A_7 + A_6 + A_5 + A_4 + A_3 - A_8 - A_9,\\
A_{11} &= \frac{-M\mathrm{Re}}{\left(1 + M\mathrm{Re}K_0\right)\left(\pi^2 + \left(1/K_0\right) + M\mathrm{Re}\right)},\\
B_2 &= \frac{A_1\mathrm{Re}\lambda\left(\lambda^2 - \pi^2\right) - \left(G\lambda_0^2/K_0\right)\mathrm{Re}^2\mathrm{Pr}^3}{\pi^2},\\
B_3 &= \frac{\mathrm{Re}^2\left(A_2\mathrm{Pr}\left(\mathrm{Re}^2\mathrm{Pr}^2 - \pi^2\right) + \left(G\lambda_0^2/K_0\right)\mathrm{Pr}^3\right)}{\mathrm{Re}^2\mathrm{Pr}\left(\mathrm{Pr}-1\right) - \left(\pi^2 + \left(1/K_0\right) + M\mathrm{Re}\right)},\\
B_4 &= \frac{\mathrm{Re}A_3\beta\left(-\beta^2 + \pi^2\right) + G\mathrm{Re}^3\mathrm{Pr}^2\left(A + B + \left(\left(d_1 - d_2\right)/\pi^2\right)\right)}{\beta^2 - \mathrm{Re}\beta - \left(\pi^2 + \left(1/K_0\right) + M\mathrm{Re}\right)},\\
B_5 &= \frac{A_4\mathrm{Re}\left(d_1 - \mathrm{RePr}\right)\left[\left(d_1 - \mathrm{RePr}\right)^2 - \pi^2\right] + AG\mathrm{Re}^3\mathrm{Pr}^2 + G\lambda_0 d_2\mathrm{RePr}\left(-1 + \mathrm{Re}^2\mathrm{Pr}^2\left(1 + \lambda_0\mathrm{Pr}\right)\right)}{\left(d_1 - \ \mathrm{RePr}\right)^2 + \mathrm{Re}\left(d_1 - \mathrm{RePr}\right) - \left(\pi^2 + \left(1/K_0\right) + M\mathrm{Re}\right)},\\
B_6 &= \frac{A_5\mathrm{Re}\left(d_2 - \mathrm{RePr}\right)\left[\left(d_2 - \mathrm{RePr}\right)^2 - \pi^2\right] + BG\mathrm{Re}^3\mathrm{Pr}^2 + G\lambda_0 d_1\mathrm{RePr}\left(1 - \mathrm{Re}^2\mathrm{Pr}^2\left(1 + \lambda_0\mathrm{Pr}\right)\right)}{\left(d_2 - \ \mathrm{RePr}\right)^2 + \mathrm{Re}\left(d_2 - \mathrm{RePr}\right) - \left(\pi^2 + \left(1/K_0\right) + M\mathrm{Re}\right)},\\
B_7 &= \frac{A_6\mathrm{Re}^2\mathrm{Pr}\left(\pi^2 - \mathrm{Re}^2\mathrm{Pr}^2\right) + G\mathrm{Re}^3\mathrm{Pr}^2\left(\left(d_1 - d_2\right)/\pi^2\right) + G\lambda_0\left(d_1 - d_2\right)\mathrm{RePr}\left(-1 + \mathrm{Re}^2\mathrm{Pr}^2\left(1 + \lambda_0\mathrm{Pr}\right)\right)}{\mathrm{Re}^2\mathrm{Pr}\left(\mathrm{Pr}-1\right) - \left(\pi^2 + \left(1/K_0\right) + M\mathrm{Re}\right)},\\
B_8 &= \frac{A_7\mathrm{Re}\left(d_1 - \lambda\right)\left(\left(d_1 - \lambda\right)^2 - \pi^2\right) + \lambda d_2\left[\left(G\lambda_0 - \left(1/\left(1 + K_0 M\mathrm{Re}\right)\right)\right)\left(1 - \lambda^2\right) - G\lambda_0^2 R_e^2\mathrm{Pr}^3\right]}{\left(d_1 - \ \lambda\right)^2 + \mathrm{Re}\left(d_1 - \lambda\right) - \left(\pi^2 + \left(1/K_0\right) + M\mathrm{Re}\right)},\\
B_9 &= \frac{A_8\mathrm{Re}\left(d_2 - \lambda\right)\left(-\left(d_2 - \lambda\right)^2 + \pi^2\right) + \lambda d_1\left[\left(G\lambda_0 - \left(1/\left(1 + K_0 M\mathrm{Re}\right)\right)\right)\left(\lambda^2 - 1\right) + G\lambda_0^2\mathrm{Re}^2\mathrm{Pr}^3\right]}{\left(d_2 - \ \lambda\right)^2 + \mathrm{Re}\left(d_2 - \lambda\right) - \left(\pi^2 + \left(1/K_0\right) + M\mathrm{Re}\right)},\\
B_{10} &= \frac{A_9\mathrm{Re}\lambda\left(\lambda^2 - \pi^2\right) + \lambda\left(d_1 - d_2\right)\left[\left(G\lambda_0 - \left(1/\left(1 + K_0 M\mathrm{Re}\right)\right)\right)\left(-\lambda^2 + 1\right) - G\lambda_0^2\mathrm{Re}^2\mathrm{Pr}^3\right]}{\pi^2},\\
B_{11} &= B_9 + B_8 + B_7 + B_6 + B_5 + B_4 - B_{10}.
\end{aligned}
\tag{58}
$$

3.6. Skin Friction Coefficients. The important physical quantity, skin friction components, can be achieved after obtaining the velocity field. In x-direction, the nondimensional skin friction component is given by

$$\tau_x^{\triangleright} = \frac{\tau_{yx}}{\rho U V_0} = \frac{\nu}{V_0 l}\left(\frac{\partial u}{\partial y}\right)_{y=0}. \tag{59}$$

We obtain the following result after omitting the symbol of "$\triangleright$" to make it easy:

$$\tau_x = S_0 + \varepsilon S_1\left(\mathrm{Re}, \mathrm{Pr}, G, K_0, L, M\right)\cos \pi z, \tag{60}$$

where

$$S_0 = \frac{1}{\mathrm{Re}}\left|\frac{\mathrm{d}u_0}{\mathrm{d}y}\right|_{y=0} - L\left|\frac{\mathrm{d}^2 u_0}{\mathrm{d}y^2}\right|_{y=0},$$
$$S_1\left(\mathrm{Re}, \mathrm{Pr}, G, K_0, L, M\right) = \frac{1}{\mathrm{Re}}\left|\frac{\mathrm{d}u_{11}}{\mathrm{d}y}\right|_{y=0} - L\left|\frac{\mathrm{d}^2 u_{11}}{\mathrm{d}y^2}\right|_{y=0}. \tag{61}$$

Similarly, in the z-direction the nondimensional skin friction component is

$$\tau_z = \frac{\tau_{yz}}{(\mu V/l)} = \left|\frac{\partial w}{\partial y}\right|_{y=0} + L\mathrm{Re}\left|\nu\frac{\partial^2 w}{\partial y^2}\right|_{y=0}$$
$$= -\varepsilon S_2\left(\mathrm{Re}, L, K_0, M\right)\sin \pi z, \tag{62}$$

where

$$S_2\left(\mathrm{Re}, L, K_0, M\right) = \frac{(1+L)d_1 d_2}{\pi\left(\pi^2 K_0 + 1\right)}\left(-1 + L\mathrm{Re}\left(d_1 + d_2\right)\right). \tag{63}$$

3.7. Heat Flux. After getting the temperature distribution, we may get The Nusselt number, Nu, from the temperature field.

$$\mathrm{Nu} = \frac{-q}{\rho V_0 c_p\left(T_w - T_\infty\right)}. \tag{64}$$

Getting nondimensional form and after simplifying the resulting equation, we have

$$\mathrm{Nu} = \frac{k_t}{\rho V_0 c_p l}\left(\frac{\partial \theta}{\partial y}\right)_{y=0} = \frac{1}{\mathrm{RePr}}\left(\frac{\mathrm{d}\theta_0}{\mathrm{d}y} + \varepsilon\frac{\partial \theta_1}{\partial y}\right)_{y=0}$$
$$= \mathrm{Nu}_0 + \varepsilon f_3\left(\mathrm{Re}, \mathrm{Pr}, K_0, M\right)\cos \pi z, \tag{65}$$

where

$$\mathrm{Nu}_0 = -1,$$
$$S_3\left(\mathrm{Re}, \mathrm{Pr}, K_0, M\right) = \frac{\mathrm{Re}pr\,(1+L)}{\left(d_1 - d_2\right)\left(\pi^2 K_0 + 1\right)}\left[-\beta\left(A + B + \frac{d_1 - d_2}{\pi^2}\right) + A\left(d_1 - R_e\mathrm{Pr}\right) + B\left(d_2 - \mathrm{RePr}\right) - \left(\frac{d_1 - d_2}{\pi^2}\right)\mathrm{RePr}\right]. \tag{66}$$

4. Results and Discussion

This effort reveals the mathematical modeling and theoretical analysis of a steady flow of second-grade fluid in three dimensions through a medium (porous) with periodic permeability and heat transfer with the existence of magnetic field applied normal to plate. With the help of regular perturbation method, analytical solutions for velocity field, pressure, heat flux, and skin friction are attained. The consequences of nondimensional parameters such as Prandtl number, elastic parameter, Reynolds number, Grashof number, magnetic parameter, and permeability parameter, $\mathrm{Pr}, L, \mathrm{Re}, G, M$, and K_0, respectively, on the obtained physical quantities are envisioned graphically.

In this regard, Figure 2 depicts the result of permeability parameter K_0 on temperature distribution, velocity components, and pressure when all other nondimensional physical parameters are static ($L = 0.01, \mathrm{Pr} = 7, \mathrm{Re} = 1, G = 1, M = 1, \varepsilon = 0.01, z = 0$) except K_0, the permeability parameter. Figure 2(a) illustrates the influence of K_0 on the temperature distribution. Here, we acquired that temperature distribution weakly depends on permeability parameter K_0. On the other hand, Figure 2(b) depicts that, near the plate, increase in permeability parameter K_0 causes increasing the pressure and at the free surface it reaches its maximum value. It is viewed from Figure 2(c) that the increase of permeability parameter K_0 leads to decrease in the main flow velocity component u. Minimum value of the velocity component occurs at the lower boundary and the maximum value of the velocity component occurs at upper boundary. Approximately, the same consequences of permeability parameter K_0 are observed in Figure 2(d) on the secondary flow velocity component v. It is detected from Figure 3(e) that velocity component w near the plate increases exponentially for a fixed value of K_0 and attains its maximum height by obtaining parabolic profile here, then decreases sharply, and alternately approaches to zero as $y \longrightarrow \infty$. It can also be observed easily that w decreases with the increase of permeability K_0.

Next, Figure 3 depicts impact of Re on θ, temperature distribution, pressure, and the components of velocity field. The impact of Re on the temperature distribution is demonstrated in

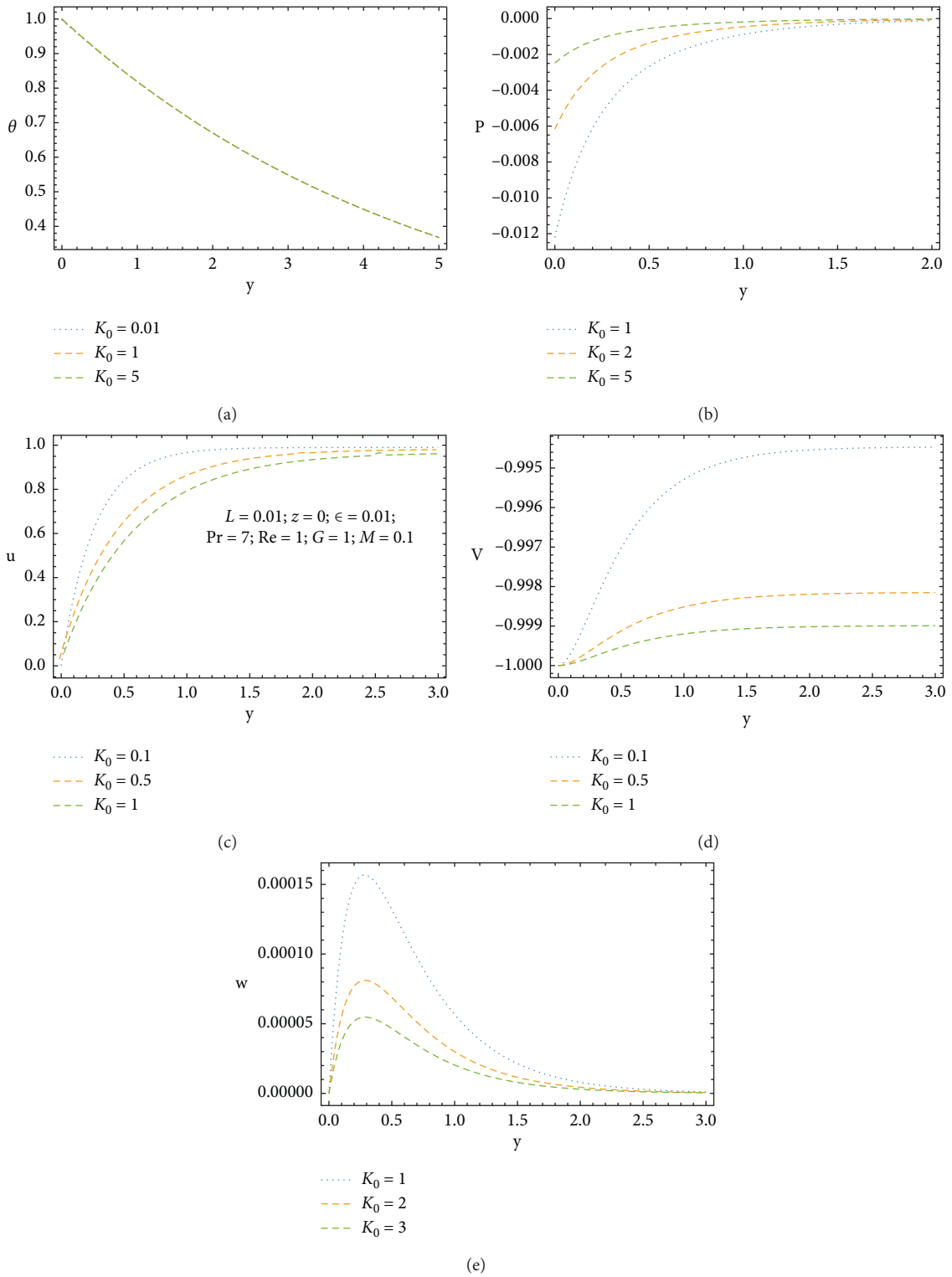

Figure 2: Impact of permeability parameter on temperature distribution, pressure, and velocity field. (a) Temperature field θ. (b) Pressure p. (c) Velocity component u. (d) Velocity component v. (e) Velocity component w.

Figure 3(a). It is noted that as we increase Reynolds number Re, the thermal boundary layer starts to decline. Figure 3(b) shows that pressure increases near the plate due to the increment of Re. Physically, it can be said that inertial forces are dominant near the plate over viscous forces. At the free surface, pressure has its maximum value. It is analyzed (Figure 3(c)) that the increment in Re causes increasing u, the main flow velocity component, and also for each value of Re the main flow velocity component u reaches its maximum value at the boundary level. Moreover, the thickness of boundary layer decreases as Reynolds number

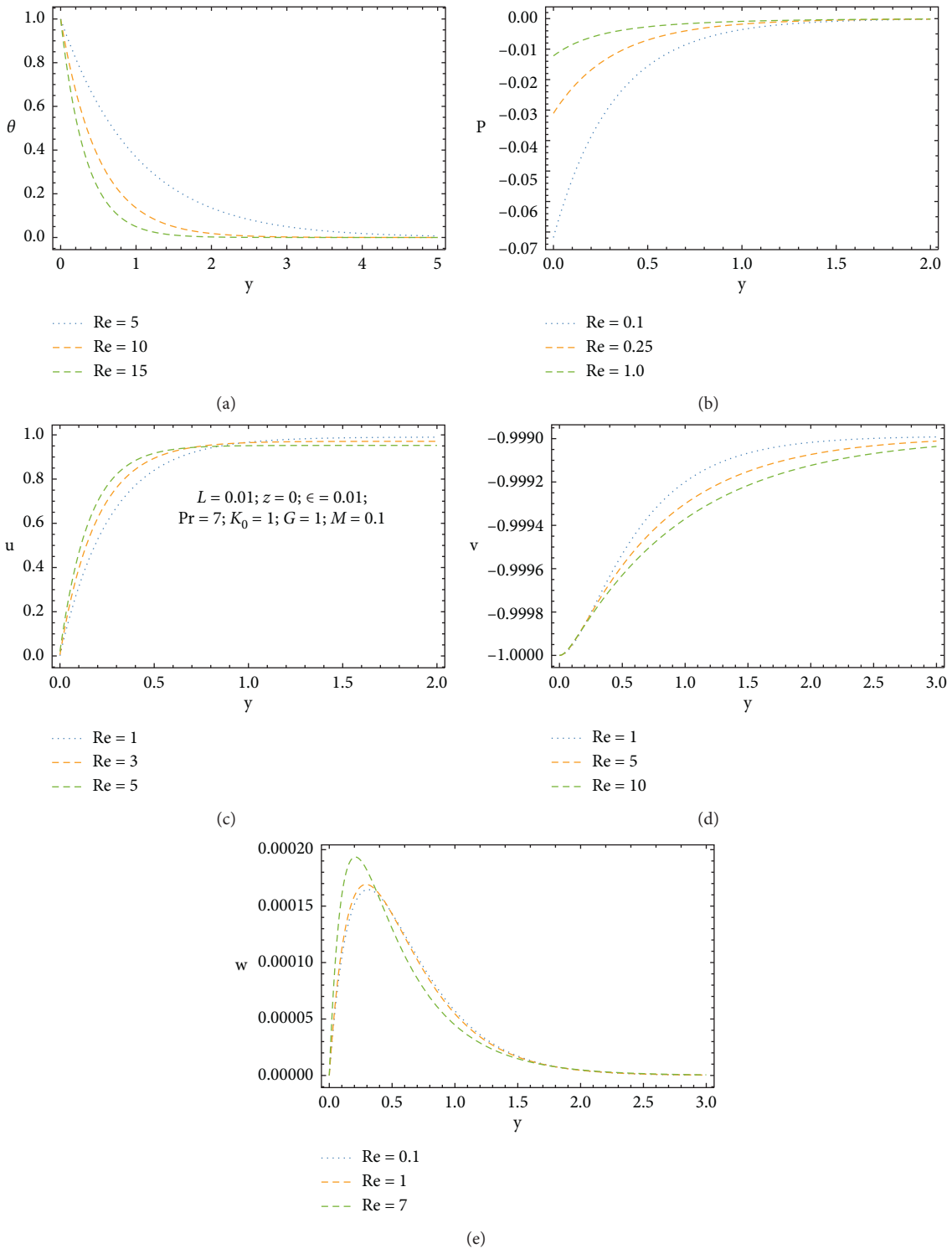

FIGURE 3: Impact of Reynolds number on temperature distribution, pressure, and velocity field. (a) Temperature field θ. (b) Pressure p. (c) Velocity component u. (d) Velocity component v. (e) Velocity component w.

increases, and the increase of Re also causes decreasing the magnitude of velocity component v (Figure 3(d)) which is naturally true with the existence of magnetic field $\vec{B}_0$. It is detected from Figure 3(e) that velocity component w near the plate increases exponentially for a fixed value of Re and attains its maximum height by making parabolic profile here and then speedily decreases, and at last $w \longrightarrow 0$ as $y \longrightarrow \infty$. It is clearly noted that w increases due to an increment of Re.

Figure 4 exhibits the impact of M on temperature distribution, pressure, and velocity components when all nondimensional parameters are fixed except magnetic parameter. Figure 4(a) demonstrates the impact of M on

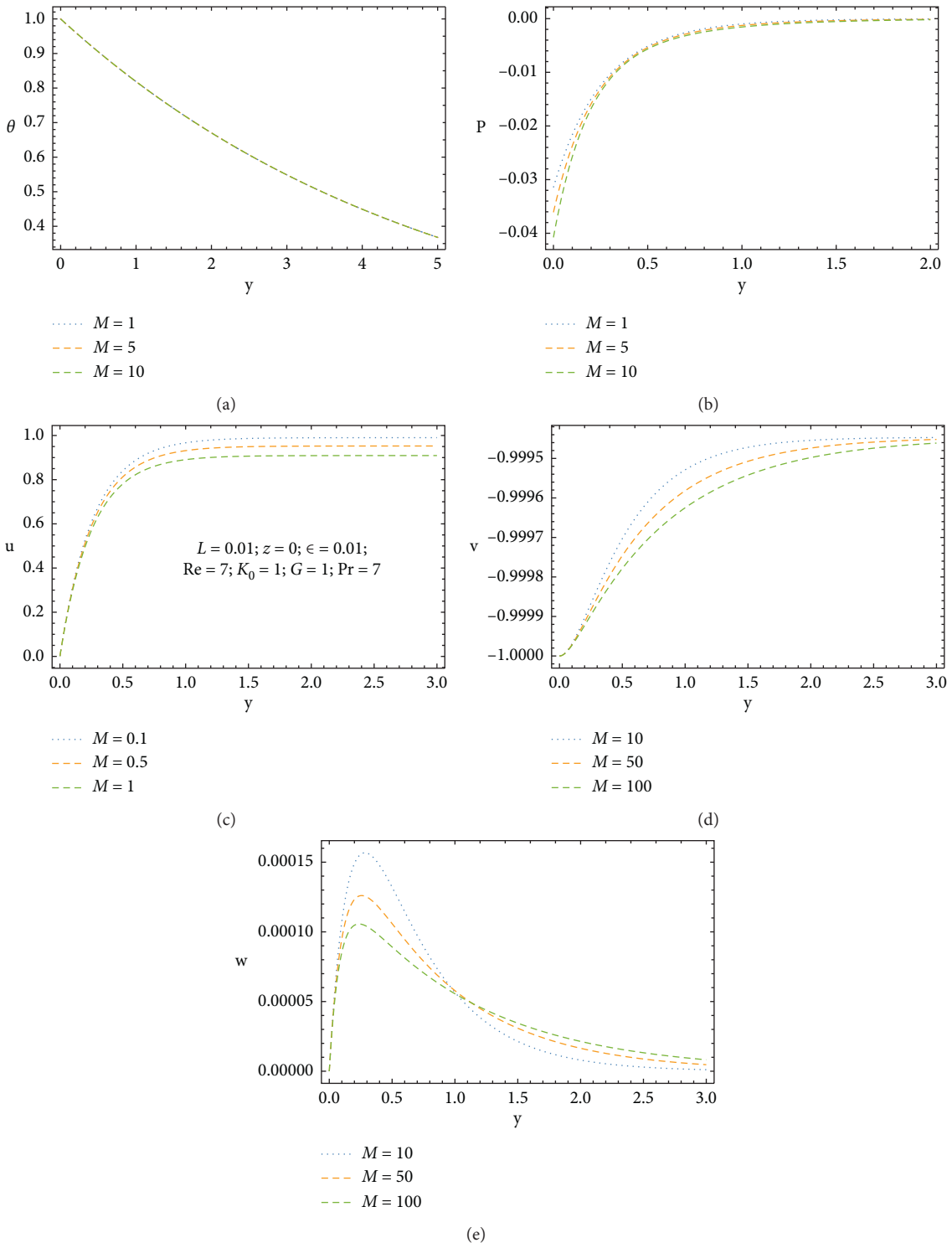

Figure 4: Impact of magnetic parameter on temperature field, pressure, and velocity field. (a) Temperature field θ. (b) Pressure p. (c) Velocity component u. (d) Velocity component v. (e) Velocity component w.

temperature distribution which illustrates that temperature distribution weakly depends on magnetic parameter M. Figure 4(b) displays that pressure decreases with an enhancement in M and reaches its maximum value at the free surface. It is investigated further by Figure 4(c) that main flow velocity component u decreases when parameter M is enhanced. Minimum value of the velocity component occurs at the lower boundary and the maximum value of the velocity component takes place at upper boundary. The same impact of magnetic parameter M on v is observed from Figure 4(d). It is viewed from Figure 4(e) that near the plate velocity component w

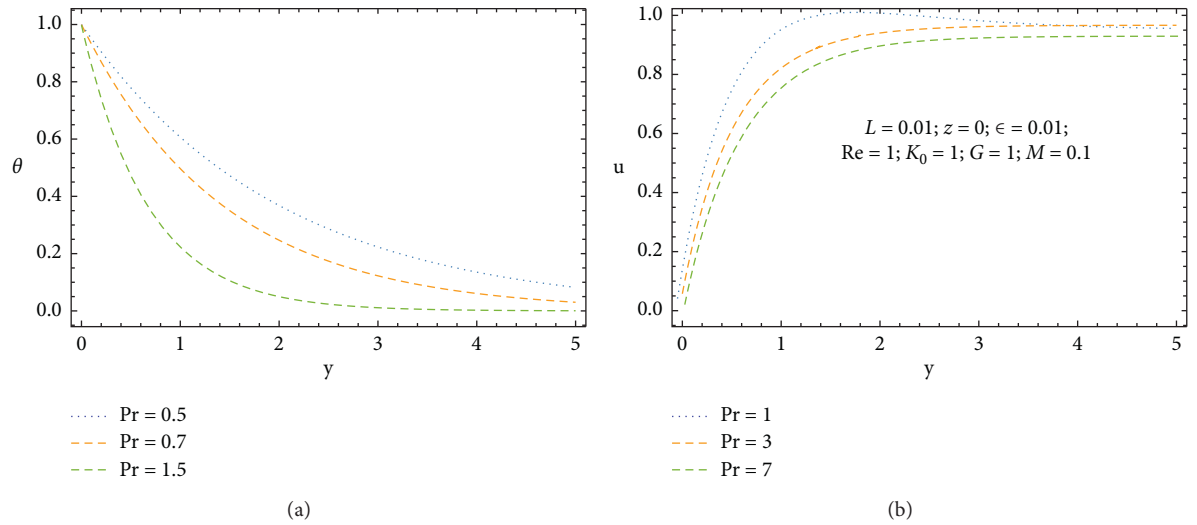

Figure 5: Impact of Prandtl number on temperature field and velocity component. (a) Temperature field. (b) Velocity component u.

increases exponentially for a fixed value of magnetic parameter M and w approaches its maximum value by making parabolic profile here; afterwards, it decreases quickly and $w \longrightarrow 0$ for $y \longrightarrow \infty$. Clearly, it can be checked that w starts to decrease by increasing the values of M.

The impact of Prandtl number on temperature field and main flow velocity component u is elaborated in Figure 5. It is obvious in Figure 5(a) that the fluid temperature reduces by the enhancement of Pr, Prandtl number, and this behavior of Pr reduces the thickness of thermal boundary layer. Actually, when we increase the Prandtl number, there exists a low thermal conductivity in fluid which causes reducing thermal layer thickness. Thus, the graphical observation of problem from this figure absolutely agrees with the physical principle that the increase of Pr causes decrease in boundary layer thickness. Figure 5(b) shows that with an increment of Prandtl number the velocity component u starts to decrease.

Figure 6 reveals the impact of elastic parameter L on temperature field, pressure, and velocity components when all other nondimensional parameters are fixed except elastic parameter. Here, it is viewed from Figure 6(a) that the influence of L on the temperature distribution is the same as K_0. Here, again we acquired that temperature distribution weakly depends on elastic parameter L. It is also exhibited (Figure 6(b)) here clearly that the pressure starts to increase by an increase in L, which is evident of above theory, because of the fluid thickness. Figure 6(c) shows that main flow velocity component u starts to decrease with the increase of non-Newtonian parameter L which is quite obvious physically as increase in non-Newtonian parameter L causes greater thickening of fluid that produces reduction in the velocity. The impact of L from Figure 6(d) on v is observed that minimum value of the velocity component occurs at the lower boundary and the maximum value of the velocity component takes place at upper boundary. It is viewed from Figure 6(e) that near the plate velocity component w increases exponentially for a fixed value of L and it decreases quickly after making parabolic profile; then $w \longrightarrow 0$ for $y \longrightarrow \infty$. It can be seen that w starts to increase by increasing the values of L.

As for the Figure 7, it perceives the impact of Grashof number that is free convective parameter on u. This effect shows the cooling of the plate that happens due to the greater Grashof number. The figure elaborates that the velocity component of main flow u starts to increase with an increase of Grashof number G which leads to the high cooling of the medium.

Further, in Figure 8, the dimensionless skin friction component along the x–axis is depicted for distinct values of L, M K_0, G, and Pr through the direction of main flow and against Reynolds number. It is observed in all cases (Figures 8(a), 8(c), 8(d), and 8(e)) that with an increase in Reynolds number Re the skin friction is imposed by the plate on the fluid, which increases with the increase of each of these dimensionless parameters. It is worth mentioning that the skin friction is zero for $L = 0.1$. However, permeability parameter K_0 has an inverse effect shown in Figure 8(b).

Figure 9 is framed for nondimensional component of skin friction along the secondary flow direction for distinct values of L, M, and K_0 against Reynolds number. In both cases (Figures 9(a) and 9(b)), it is perceived that the increase in Re originates the increase in component of skin friction. With the increase in either of the parameters L and M, the

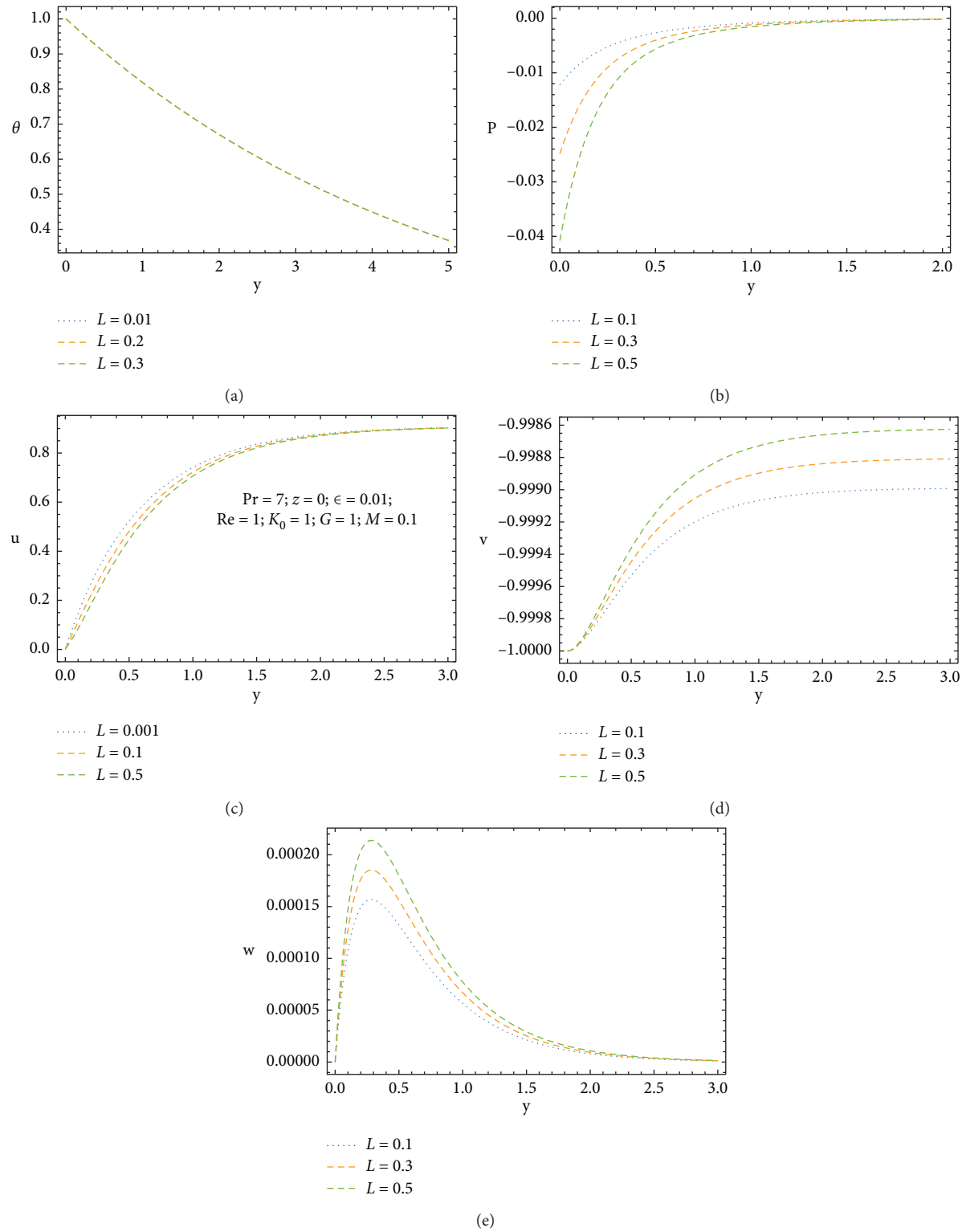

Figure 6: Impact of non-Newtonian parameter on temperature field, pressure, and velocity field. (a) Temperature field. (b) Pressure. (c) Velocity component u. (d) Velocity component v. (e) Velocity component w.

skin friction increases; however, permeability parameter K_0 has an inverse effect (Figure 9(c)).

In Figure 10, variation of dimensionless coefficient of heat transfer for the different values of L, Pr, M, and K_0 is demonstrated against Reynolds number. It is evident that coefficient of heat transfer is enhanced with an increase in either of the parameter L, Pr, and M. In contrast, the heat transfer coefficient decreases by increasing K_0.

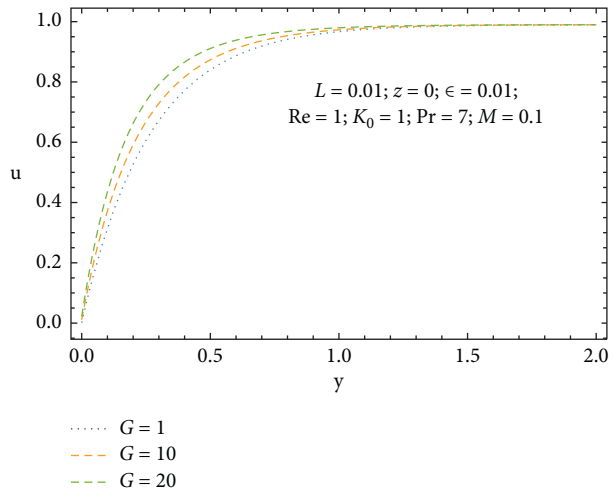

Figure 7: Main flow velocity with the impact of Grashof number.

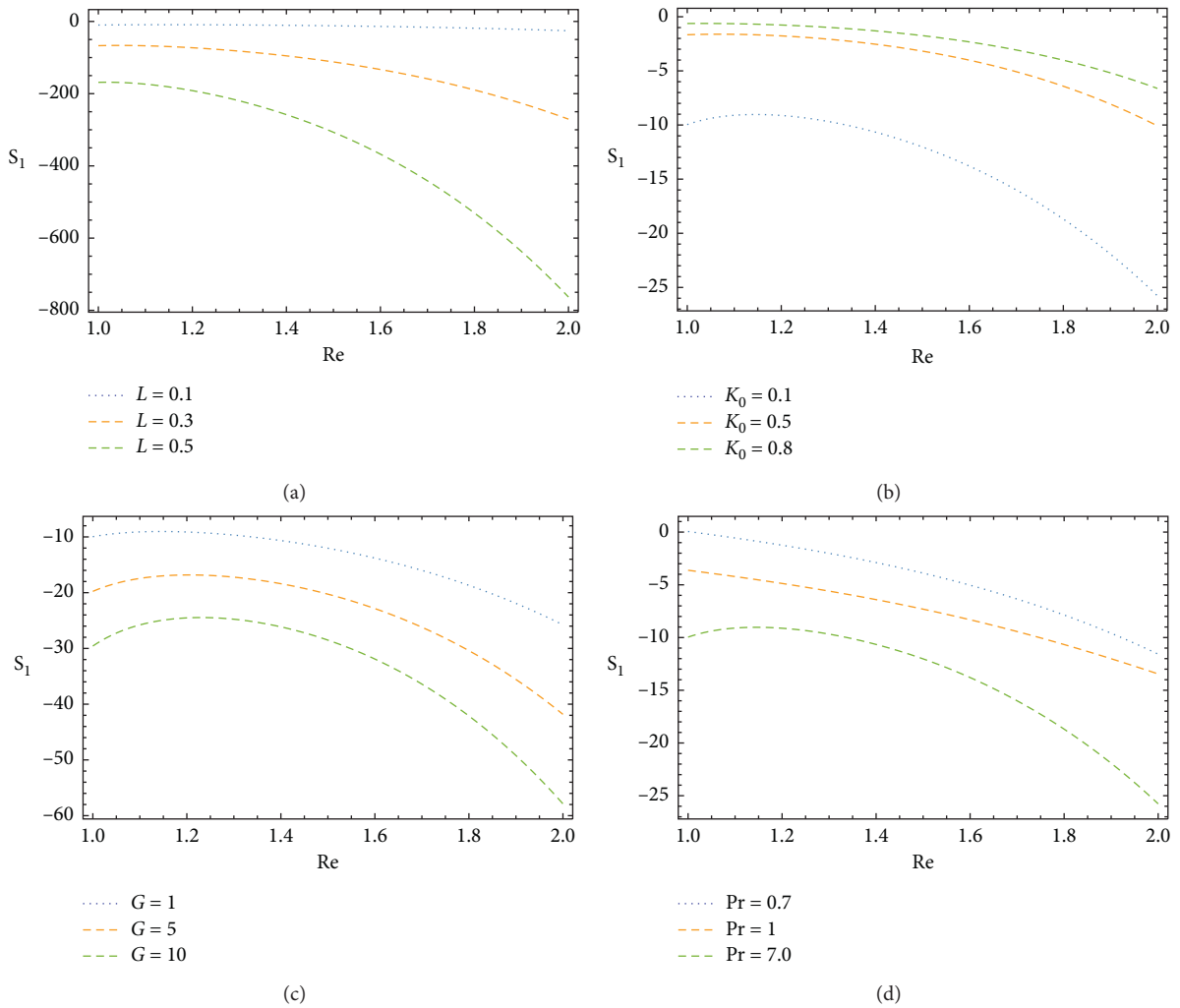

Figure 8: Continued.

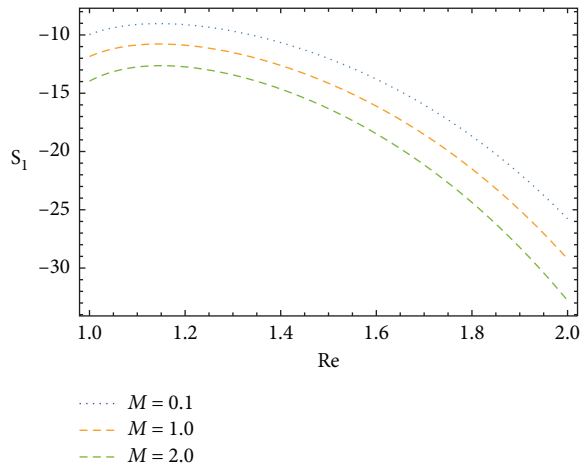

(e)

Figure 8: Impact of dimensionless parameters on skin friction component along x-axis. (a) Effect of elastic parameter. (b) Effect of permeability parameter. (c) Effect of Grashof number. (d) Effect of Prandtl number. (e) Effect of magnetic parameter.

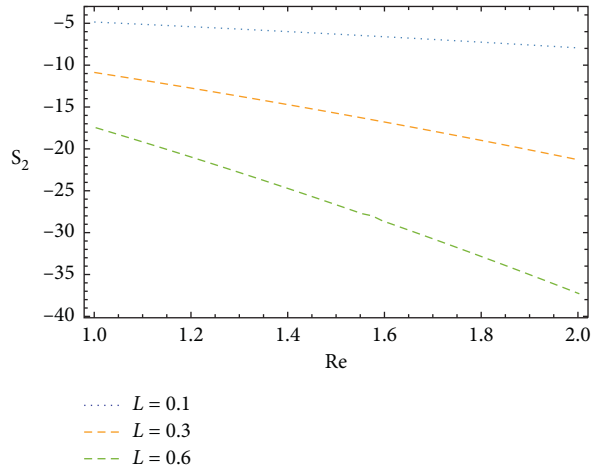

(a)

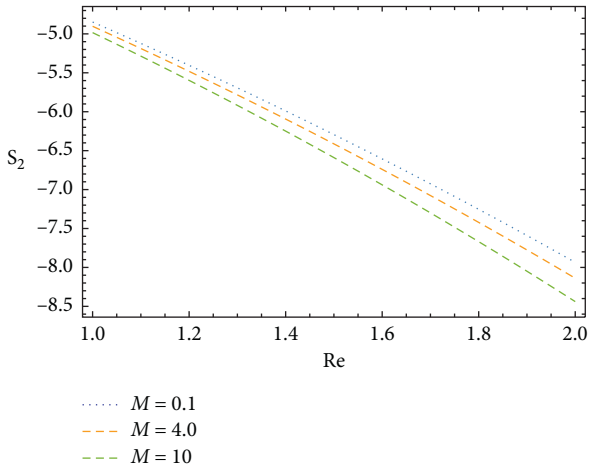

(b)

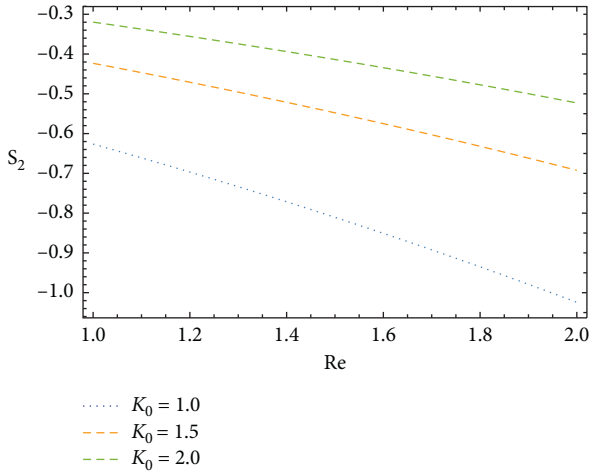

(c)

Figure 9: Impact of dimensionless parameters on skin friction component along z-axis. (a) Effect of elastic parameter. (b) Effect of magnetic parameter. (c) Effect of magnetic parameter.

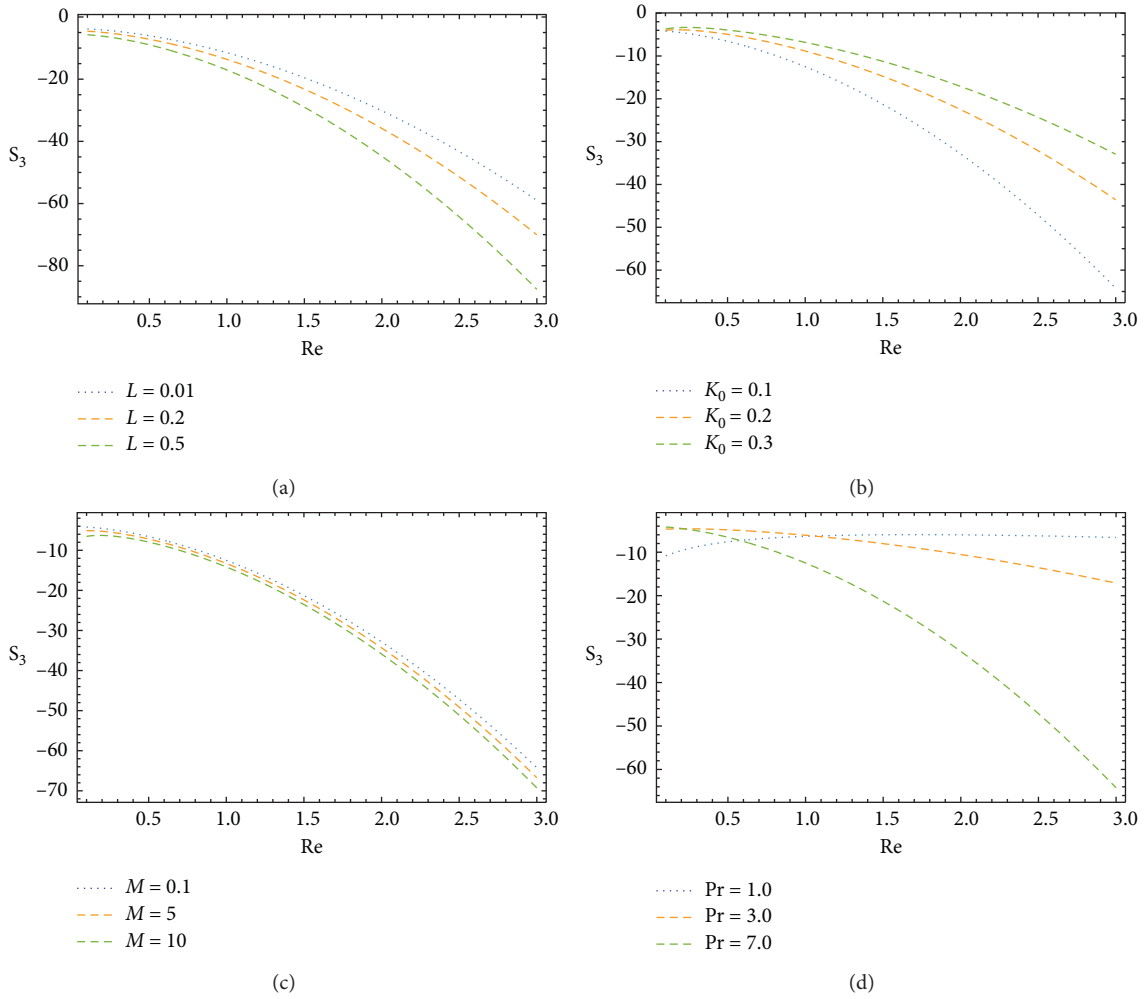

FIGURE 10: Impact of dimensionless parameters on Nusselt number. (a) Effect of elastic parameter. (b) Effect of permeability parameter. (c) Effect of magnetic parameter. (d) Effect of Prandtl number.

5. Final Remarks

The main outcomes observed in the article are described in the following for the focus of reader:

(i) Magnetic field reduces the velocity field.

(ii) High cooling of the medium causes an increase in main flow velocity component.

(iii) The temperature distribution weakly depends upon the Hartmann number.

(iv) The fluid pressure rises due to increase in values of non-Newtonian parameter.

(v) The skin friction components increase as the elastic parameter increases. It is also interesting to note that the skin friction component along the main flow direction reduces to zero for $L = 0.1$.

(vi) Reynolds number causes controlling boundary layer thickness. It also provides a tool to control thermal boundary layer.

(vii) Permeability plays a role of root to minimize the components of skin friction.

(viii) The plate friction decreases due to increase in permeability parameter.

(ix) It is observed that permeability parameter weakly depends on temperature field.

(x) It is a noteworthy evaluation that the solutions of [21] are retrieved in the absence of M as well as results of [6] recaptured while eliminating both M and L.

Abbreviations

$\widetilde{A_1}$, $\widetilde{A_2}$:	Rivlin–Ericksen tensors
A_i; $i = 1, 2, \ldots, 11$:	Constants of integrations
B_i; $i = 2, \ldots, 11$:	Constants of integrations
$\overrightarrow{B}_0$:	A magnetic field normal to plate
A, B:	Constants involved in solution
c_p:	Specific heat (at constant pressure) (J/K.kg)
M:	Magnetic parameter
g:	Gravity (m/s^2)
G:	Grashof number

$\widetilde{I}$: Tensor (unit)
k_t: Conductivity (thermal) (W/(m.K))
K_0: Mean permeability (m^2)
l: Length of wave (m)
$\overrightarrow{J}$: Electric current density
L: Parameter (elastic)
p and p_∞: Pressures (variable and constant) ($Pa = N/m^2$)
Nu: Nusselt number
Pr: Prandtl number
$\overrightarrow{q}$: Flux (heat) (kg/s^3)
Re: Reynolds number
T: Temperature (K)
$T_w; T_\infty$: Temperatures (at wall and free stream) (K)
u, v, w: Velocity components (m/s)
$U; V_0$: Constant velocities (free stream velocity; suction velocity) (m/s)
$\overrightarrow{V}$: Velocity field (m/s)
x, y, z: Coordinate axes (m).

Greek letters

α: Suction parameter
β_0: Thermal expansion coefficient (1/K)
$\beta, \lambda, \lambda_0, \lambda_1$: Constants involved in solution
α_1, α_2: Material constants
ε: Permeability variation amplitude (m)
ρ: Density (kg/m^3)
μ; ν: Viscosity (dynamic) (kg/(m.s)); viscosity (kinematic) (m^2/s)
μ_m: Magnetic permeability
ϱ: Energy (internal) per unit mass (J/kg)
$\widetilde{\tau}$: Tensor for Cauchy stress (N/m^2)
∇: Vector operator (1/m)
τ_x: x−component of skin friction (N/m^2)
τ_z: z−component of skin friction (N/m^2).

Data Availability

All the supporting data for this research to obtain the findings are included within this article.

Conflicts of Interest

All the authors declare that they have no conflicts of interest.

References

[1] A. A. Raptis, "Unsteady free convective flow through a porous medium," *International Journal of Engineering Science*, vol. 21, no. 4, pp. 345–348, 1983.

[2] A. A. Raptis and C. P. Perdikis, "Oscillatory flow through a porous medium by the presence of free convective flow," *International Journal of Engineering Science*, vol. 23, no. 1, pp. 51–55, 1985.

[3] K. D. Singh and S. K. Rana, "Three dimensional flow and heat transfer through a porous medium," *Indian Journal of Pure and Applied Mathematics*, vol. 23, no. 7, pp. 905–914, 1992.

[4] K. D. Singh and S. Kumar, "Two-dimensional unsteady free convective flow through a porous medium bounded by an infinite vertical porous plate with periodic permeability," *Journal of Mathematical and Physical Sciences*, vol. 27, pp. 141–148, 1993.

[5] K. D. Singh, K. Chand, and G. N. Verma, "Heal transfer in a three-dimensional flow through a porous medium with periodic permeability," *ZAMM-Journal of Applied Mathematics and Mechanics/Zeitschrift für Angewandte Mathematik und Mechanik*, vol. 75, no. 11, pp. 950–952, 1995.

[6] K. D. Singh and R. Sharma, "Three dimensional free convective flow and heat transfer through a porous medium with periodic permeability," *Indian Journal of Pure and Applied Mathematics*, vol. 33, no. 6, pp. 941–949, 2002.

[7] K. Vafai and H. Hadim, "Overview of current computational studies of heat transfer in porous media and their applicationsnatural and mixed convection," *Advances in Numerical Heat Transfer*, vol. 2, pp. 331–369, 2000.

[8] N. C. Jain, B. Sharma, and D. K. Vijay, "Three dimensional free convective flow heat transfer flow through a porous medium with periodic permeability in slip flow regime," *Journal of Heat and Mass Transfer*, vol. 28, no. 1, pp. 29–44, 2006.

[9] N. Ahmed, "Magnetic field effect on a three-dimensional mixed convective flow with mass transfer along an infinite vertical porous plate," *International Journal of Engineering, Science and Technology*, vol. 2, no. 2, pp. 117–135, 2010.

[10] P. R. Reddy, K. Srihari, and S. R. Reddy, "Combined heat and mass transfer in MHD three-dimensional porous flow with periodic permeability heat absorption," *International Journal of Mechanical Engineering & Technology*, vol. 3, no. 2, pp. 573–593, 2012.

[11] C.-Y. Cheng, "Soret and dufour effects on mixed convection heat and mass transfer from a vertical wedge in a porous medium with constant wall temperature and concentration," *Transport in Porous Media*, vol. 94, no. 1, pp. 123–132, 2012.

[12] R. A. Shah, S. Rehman, M. Idrees, M. Ullah, and T. Abbas, "Similarity analysis of MHD flow field and heat transfer of a second grade convection flow over an unsteady stretching sheet," *Boundary Value Problems*, vol. 2017, no. 1, p. 162, 2017.

[13] F. Capone1 and R. D. Luca1, "Porous MHD convection: effect of vadasz inertia term," *Transport in Porous Media*, vol. 118, no. 3, pp. 519–536, 2017.

[14] M. VeeraKrishna, G. S. Reddy, and A. J. Chamkha, "Hall effects on unsteady MHD oscillatory free convective flow of second grade fluid through porous medium between two vertical plates," *Physics of Fluids*, vol. 30, no. 2, p. 23106, 2018.

[15] S. Baag, M. R. Acharya, G. C. Dash, and S. R. Mishra, "MHD flow of a visco-elastic fluid through a porous medium between infinite parallel plates with time dependent suction," *Journal of Hydrodynamics*, vol. 27, no. 5, Article ID 840847, 2015.

[16] S. R. Mishra, P. K. Pattnaik, M. M. Bhatti, and T. Abbas, "Analysis of heat and mass transfer with MHD and chemical reaction effects on viscoelastic fluid over a stretching sheet," *Indian Journal of Physics*, vol. 91, no. 10, Article ID 12191227, 2017.

[17] S. R. Mishra, R. S. Tripathy, and G. C. Dash, "MHD visco-elastic fluid flow through porous medium over a stretching sheet in the presence of non-uniform heat source/sink," *Rendiconti del Circolo Matematico di Palermo Series*, vol. 2, no. 1, Article ID 129143, 2018.

[18] G. S. Seth, A. Bhattacharyya, and M. K. Mishra, "Study of partial slip mechanism on free convection flow of viscoelastic fluid past a nonlinearly stretching surface," *Computational Thermal Sciences*, vol. 11, pp. 107–119, 2018.

[19] A. Bhattacharyya, G. S. Seth, and R. Kumar, "Modeling of viscoelastic fluid flow past a non-linearly stretching surface with convective heat transfer: OHAM analysis," in *Proceedings of the International Conference On Mathematical Modelling And Scientific Computation*, pp. 297–312, Springer, Singapore, February 2018.

[20] G. S. Seth, A. Bhattacharyya, R. Kumar, and M. K. Mishra, "Modeling and numerical simulation of hydromagnetic natural convection casson fluid flow with nth-order chemical reaction and Newtonian heating in porous medium," *Journal of Porous Media*, vol. 22, no. 9, pp. 1141–1157, 2019.

[21] M. A. Rana and A. Latif, "Three-DimensionalFree convective flow of a second GradeFluid through a porous medium with periodic permeability and heat transfer," *Boundary Value Problems*, vol. 2019, no. 1, p. 44, 2019.

[22] A. Latif and M. A. Rana, "Analysis of free convective jeffery's fluid with periodic permeability and cattaneo-christov heat transfer," *IFAC-PapersOnLine*, vol. 51, no. 30, pp. 155–160, 2018.

[23] M. Kar and G. C. Dash, "Three-dimensional free convection MHD flow in a vertical channel through a porous medium with heat source and chemical reaction," *Journal of Engineering Thermophysics*, vol. 22, no. 3, Article ID 203215, 2013.

[24] M. V. Krishna and G. S. Reddy, "Unsteady MHD convective flow of Second grade fluid through a porous medium in a Rotating parallel plate channel with temperature dependent source," *Conference Series: Materials Science and Engineering*, vol. 149, no. 1, p. 12216, 2016.

[25] B. C. Shekar, N. Kishan, and A. J. Chamkha, "Soret and Dufour effects on MHD natural convective heat and solute transfer in a fluid-saturated porous cavity," *Journal of Porous Media*, vol. 19, no. 8, Article ID 669686, 2016.

[26] M. Shoaib and R. Akhtar, "A novel design of MHD three-dimensional flow of second grade fluid past a porous plate," *Mathematical Problems in Engineering*, vol. 2019, Article ID 2584397, 2019.

[27] S. Prema, B. M. Shankar, and K. N. Seetharamu, "Convection heat transfer in a porous medium saturated with an Oldroyd B fluid-a review," *International Journal of Physics: Conference Series*, vol. 1473, p. 12029, 2020.

[28] F. Arpino, G. Cortellessa, and A. Mauro, "Transient thermal analysis of natural convection in porous and partially porous cavities," *Numerical Heat Transfer, Part A: Applications*, vol. 67, no. 6, pp. 605–631, 2015.

[29] F. Arpino and A. Carotenuto, "Transient natural convection in partially porous vertical annuli," *International Journal of Heat and Technology*, vol. 34, no. 2, pp. S512–S518, 2016.

[30] K. Khanafer and K. Vafai, "Applications of nanofluids in porous medium," *Journal of Thermal Analysis and Calorimetry*, vol. 135, no. 2, pp. 1479–1492, 2019.

[31] G. W. Sutton and A. Sherman, *Engineering Magnetohydrodynamics*, McGraw-Hill, New York, NY, USA, 1965.

[32] J. A. Sherchiff, *A Textbook of Magnetohydrodynamics*, Pergaman Press, Oxford, UK, 1965.

[33] T. Papanastasiou, G. Georgiou, and A. N. Alexandrou, *Viscous Fluid Flow*, CRC Press, Boca Raton, FL, USA, 1999.

[34] F. M. White and I. Corfield, *Viscous fluid flow*, Vol. 3, McGraw-Hill, New York, NY, USA, 2006.

[35] J. E. Dunn and R. L. Fosdick, "Thermodynamics, stability, and boundedness of fluids of complexity 2 and fluids of second grade," *Archive for Rational Mechanics and Analysis*, vol. 56, no. 3, pp. 191–252, 1974.